PROPAGATION THROUGH ELECTRICALLY COUPLED CELLS

How a Small SA Node Drives a Large Atrium

RONALD W. JOYNER* AND FRANS J. L. VAN CAPELLE‡
*Department of Physiology and Biophysics, The University of Iowa, Iowa City, Iowa 52242; and
‡Department of Experimental Cardiology, Academic Medical Center, Meibergdrees 1105-AZ, Amsterdam, The Netherlands

ABSTRACT Each normal cardiac cycle is started by an action potential that is initiated in the sino-atrial (SA) node by automaticity of the SA nodal cells. This action potential then propagates from the SA node into the surrounding atrial cells. We have done numerical simulations of electrically coupled cells to understand how a small SA node can be spontaneously active and yet be sufficiently electrically coupled to the surrounding quiescent atrial cells to initiate an action potential in the atrial cells. Our results with a simple model of two coupled cells and a more complex model of a two-dimensional sheet of cells suggest that some degree of electrical uncoupling of the cells within the SA node may be an essential design feature of the normal SA–atrial system.

INTRODUCTION

In the normal cardiac excitation sequence the action potential is initiated in the sino-atrial (SA) node and then travels through the atrial wall, the atrio-ventricular (AV) node, the Purkinje (P) system, and the ventricular (V) wall. The time course of the action potential (membrane potential as a function of time) is markedly different in different regions of the heart, with regional variation in the presence or absence of diastolic depolarization, the action potential duration (APD), and the ionic mechanism for the rising phase. When the action potential propagates from one region to another, there appear to be cells between the two regions that have an intermediate action potential waveform. For example, the region of the atrial wall containing the SA node has been extensively studied with both histological and electrophysiological techniques (see Masson-Pevet et al., 1979; 1982 for review). The overall structure consists of a small central core of leading pacemaker cells surrounded by latent pacemaker cells which with increasing distance from the central core, appear more and more like typical atrial cells with respect to their histological appearance and the recorded action potentials.

However, it has been shown (Joyner et al., 1983) that the action potential waveform recorded from a cell in an elecrical syncytium is not determined solely by the intrinsic membrane properties of that cell. The presence of electrical coupling among cells would be expected to create "transitional" action potential shapes in cells near the border zone between two distinctly different cell types. These "electrotonic" influences make it very difficult to prove that cells in a particular region are truly "transitional" in terms of their intrinsic membrane properties. Ultimately, this demonstration will require very careful regional cell isolation with comparative single cell electrical studies. Recent studies with the isolation of small groups of cells near the SA node (Kodama and Boyett, 1985) have provided evidence that a gradual spatial variation in intrinsic cellular electrical properties does exist in the rabbit SA node–atrial region.

There are many phenomena of SA node–atrial interactions that are presently unexplained. The propagation of action potentials away from the SA node is not circular. Detailed studies (Bleeker et al., 1982) show preferential conduction (higher velocity) along the axis parallel to the crista terminalis (CT). There is slow conduction toward the CT and actual propagation failure away from the CT. In addition, it has been shown that the earliest activated site can shift in location in response to application of acetylcholine and adrenaline (Mackaay et. al., 1980). These phenomena must eventually be explained by a multi-dimensional model with spatial distributions of both membrane properties and the cell–cell coupling resistances. The present work is an initial step in which we assume radial symmetry, only two types of cells, and a radial distribution of cell–cell coupling resistance and show that these features will at least allow a small SA node to successfully pace and drive a much larger atrial region.

Address correspondence to Dr Joyner.

METHODS

We have previously described methods for the numerical simulation of action potential propagation in a one-dimensional strand of cells (Sharp and Joyner, 1980), a two-dimensional sheet of excitable cells (Joyner et al., 1975), or in a system with two coupled layers of cells (Joyner et al., 1984). Here we simulate a two-dimensional layer of cells with radial symmetry, as diagrammed in Fig. 1. The circular layer of cells is divided into a large number (M) of regions, with the width of each region being ΔA. The central region has a radius ΔA and the thickness of the sheet is T. Thus, for M regions the total radius, A_t, is $M\Delta A$. Each region represents a group of cells that are isopotential due to the assumption of circular symmetry. If the surface to volume ratio of the cells is S_v (cm^{-1}) then the membrane surface area of each region ($j = 1, 2, \ldots M$) is $S(j) = S_v \pi T (\Delta a)^2 (2j-1)$. If the combination of cytoplasmic and junctional resistance connecting a region j to region $j+1$ produces a net resistivity of R_j (Ω cm), then the actual resistance (Ω) will be defined as $R_x(j)$ and is approximately equal to $R_j/2\pi jT$. If we use (for each circular element) a membrane model in which the membrane current, conductances, and capacitance are expressed per cm^2, then these terms are simply scaled by $S(j)$ for computation at each circular element. The radial symmetry of the model preparation then allows the standard difference equation for a one-dimensional strand (Joyner et al., 1983)

$$\frac{V_{j-1} - V_j}{R_x(j-1)} - \frac{V_j - V_{j+1}}{R_x(j)} = S(j)\,[C_m(\delta V_j/\delta t) + I_j] \quad (1)$$

to be used to compute V_j for each element as a function of time. With the appropriate substitution for $S(j)$ and $R_x(j)$, this becomes

$$\frac{V_{j-1} - V_j}{R_{j-1}/[2\pi T(j-1)]} - \frac{V_j - V_{j+1}}{R_j/(2\pi Tj)} = S_v \pi T (\Delta A)^2 (2j-1)[C_m(\delta V_j/\delta t) + I_j], \quad (2)$$

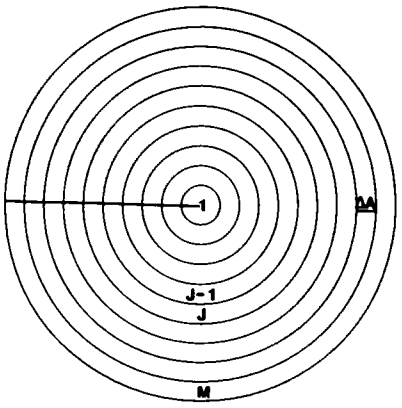

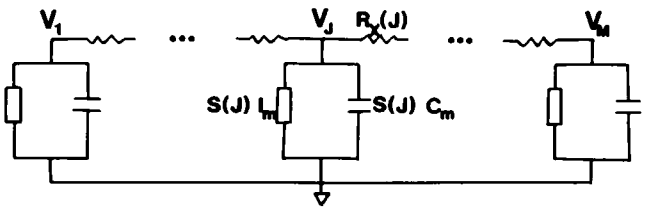

FIGURE 1 Schematic diagram of a disk model to represent a two-dimensional sheet of excitable cells, assuming radial symmetry. Concentric regions are modeled by isopotential elements, numbered 1, 2, ... M with each element consisting of membrane capacitance and a membrane ionic current function, I_m. $S(j)$ is the membrane area of the j^{th} element. $R_x(j)$ is the resistance (Ω) coupling elements j and $j+1$.

where I_j is the membrane current (mA/cm^2) computed as a function of time and voltage from the membrane model used for element j.

As in the method of Crank and Nicolson (1947), letting V_j^t be the membrane potential of element j at time t, we express $\delta V/\delta t$ as $(V_j^{t+\Delta t} - V_j^t)/\Delta t$ and substitute the average of V values at time t and time $t+\Delta t$ for the term on the left and rearrange as

$$K_j' V_{j-1}^{t+\Delta t} + [K_j + K_j' + 1]\, V_j^{t+\Delta t} - K_j V_{j+1}^{t+\Delta t} = K_j' V_{j-1}^t\,[K_j + K_j' - 1]\, V_j^t + K_j V_{j+1}^t - \Delta t\, I_j/C_m, \quad (3)$$

where

$$K_j = \Delta t j \,/\, [C_m R_j S_v (\Delta A)^2 (2j-1)]$$

and

$$K_j' = \Delta t(j-1)/[C_m R_j S_v (\Delta A)^2 (2j-1)].$$

This equation can then be solved for $V_j^{t+\Delta t}$ for $j = 1, 2, \ldots M$ at each time step by matrix methods as previously used (Moore et al., 1975). For all of the simulations we used $C_m = 1\ \mu F/cm^2$, $S_v = 5{,}000\ cm^{-1}$ (Sommer and Johnson, 1979) and a discrete time step of 5 μs. We assumed a constant value for the thickness of the disk model (T) and therefore this parameter is absent from Eq. 3 and does not affect the simulated results. Boundary conditions are treated as in our previously published one-dimensional method (Joyner et al., 1978) as "sealed ends," which simply means that, for $j = 1$, $K_j' = 0$ and, for $j = M$, $K_j = 0$. Our solution of the radial cable equations as a set of difference equations does not require an analytical solution, which would result in a singularity at j = 1 if A were to be infinitely small (Twizell, 1984).

The models we have used for the SA NODE cells (Irisawa and Noma, 1982) and for the ATRIAL cells (Beeler and Reuter, 1977) are necessarily approximations to the true intrinsic membrane properties. We modified the Beeler-Reuter model, which was developed for ventricular cells, by reducing the slow inward current by a factor of five to decrease the action potential duration to ~100 ms to correspond with the duration of rabbit atrial action potentials. Quantitatively, results from our simulations depend heavily on the effects of outward current during the diastolic period of the SA NODE model and the process of sodium channel inactivation in the ATRIAL model. Neither of these processes has been experimentally verified using these models or other available models. Our focus, in these simulations, is to investigate the effects of coupling resistance on the electrical properties of a syncytium of cells with dissimilar properties, using the membrane models chosen as the best available at this time.

RESULTS

I. SA–Atrial Interactions—Two Cells

If the SA–atrial region were successfully constructed as a discrete group of SA cells surrounded by a much larger number of atrial cells then one would certainly expect that a single SA cell would be able to pace repetitively and provide successful stimulation to a single atrial cell with some value of electrical coupling between the two cells. Before considering the results of a simulated two-dimensional layer of cells, we will first present some results for a simulated pair of isopotential membrane regions (i.e., two isopotential cells or two isopotential cell aggregates) connected by a junctional resistance. For the simulations shown in Fig. 2, we used two isopotential membrane regions coupled by a resistance R_c. For the "SA NODE" region we used the membrane model of Irisawa and Noma (1982). For the "ATRIAL" region we used the model of

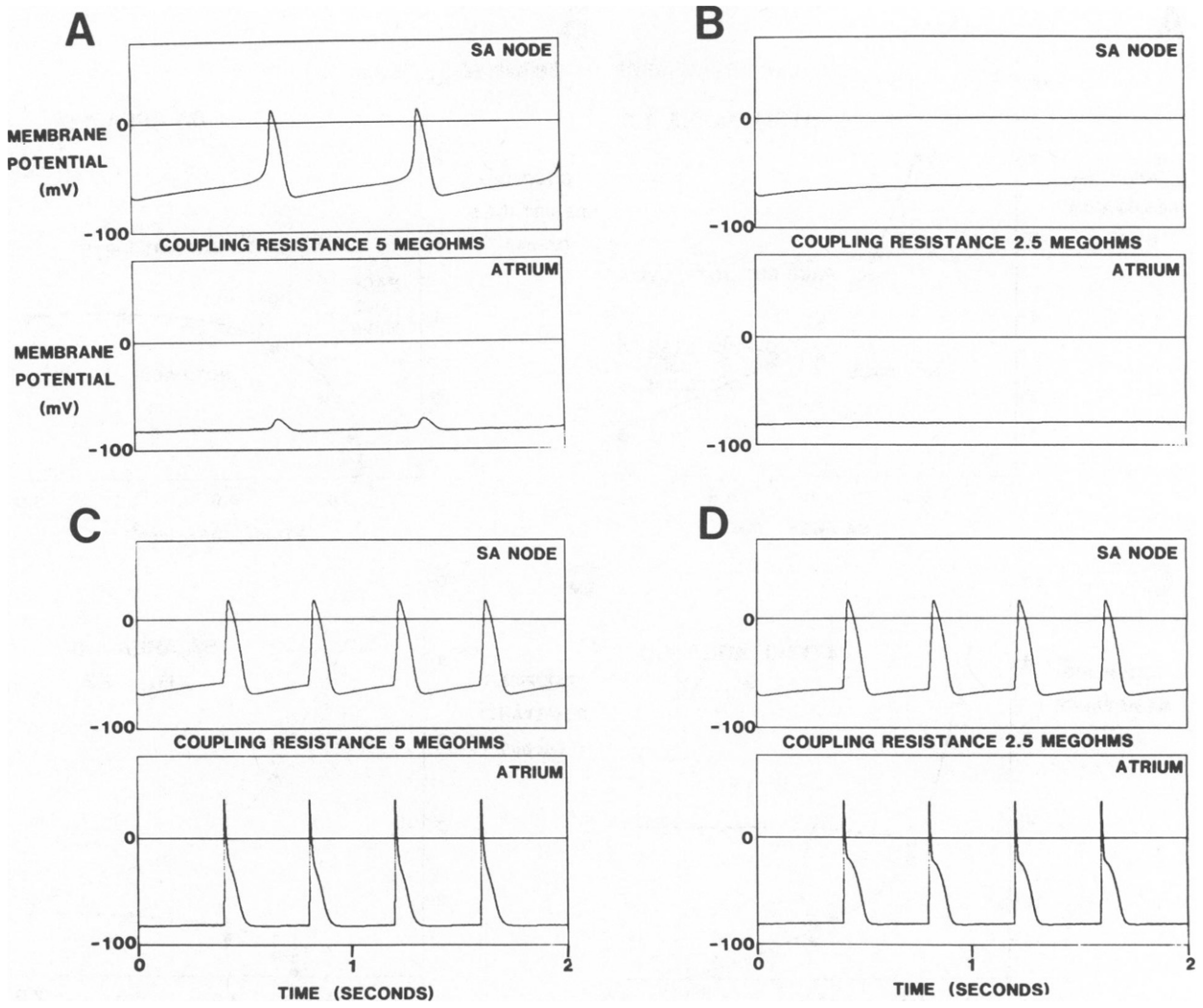

FIGURE 2 Simulated results for two electrically coupled membrane regions. In each panel, the upper trace is for the region with the SA node membrane model and the lower trace is for the region with the atrial membrane model. For all panels (*A–D*) the membrane area of each region is 1 mm^2. The coupling resistance is 5 MΩ for *A* and *C;* 2.5 MΩ for *B* and *D*. For *C* and *D* a repetitive stimulus is applied to the atrial region.

Beeler and Reuter (1977) with the only modification being a reduction in the magnitude of the conductance for the slow inward current to 20% of the standard model to produce an action potential duration of ~100 ms to correspond with atrial cell action potential duration and to shorten the refractory period to an appropriate level. *A* and *B* show the results for coupling resistance of 5 and 2.5 MΩ, with the SA node and atrial membrane areas both set to 1 mm^2. For R_c = 5 MΩ (*A*) the SA node paces but does not drive the atrium. For R_c = 2.5 MΩ (*B*) the SA node does not pace. *C* and *D* show that, if the atrium is repetitively stimulated by a small current injection (1 ms duration, 0.1μA) the SA node can be driven from the atrium at both levels of R_c.

When we systematically varied the three parameters (R_c, atrial membrane area, SA node area), we found that the coupled system could exhibit the three possible results of (*a*) SA node not pacing, (*b*) SA node pacing but not able to drive the atrium, and (*c*) SA node pacing and driving the atrium. These results are shown in Fig. 3. In *A* we show the results obtained when the atrial membrane area was fixed at 1 mm^2 while the SA node membrane area and R_c were varied. Each symbol plotted represents the results of a simulation with the filled circles indicating that the SA node did not pace, the open circles indicating that the SA node paced but did not drive the atrium, and the open triangles indicating that the SA node paced and was able to drive the atrium. From the simulations we showed that the space formed by all possible combinations of SA membrane area and R_c was divided into three regions as indicated by the solid and dashed lines. As an extension of the results shown in Fig. 2, Fig. 3 *A* shows that, if SA node and atrial membrane area are both equal to 1 mm^2, there is no value of R_c that will allow the SA node to pace and to drive the atrium. In fact, for these membrane models, the SA node membrane area must be ~1.2 times as large as the

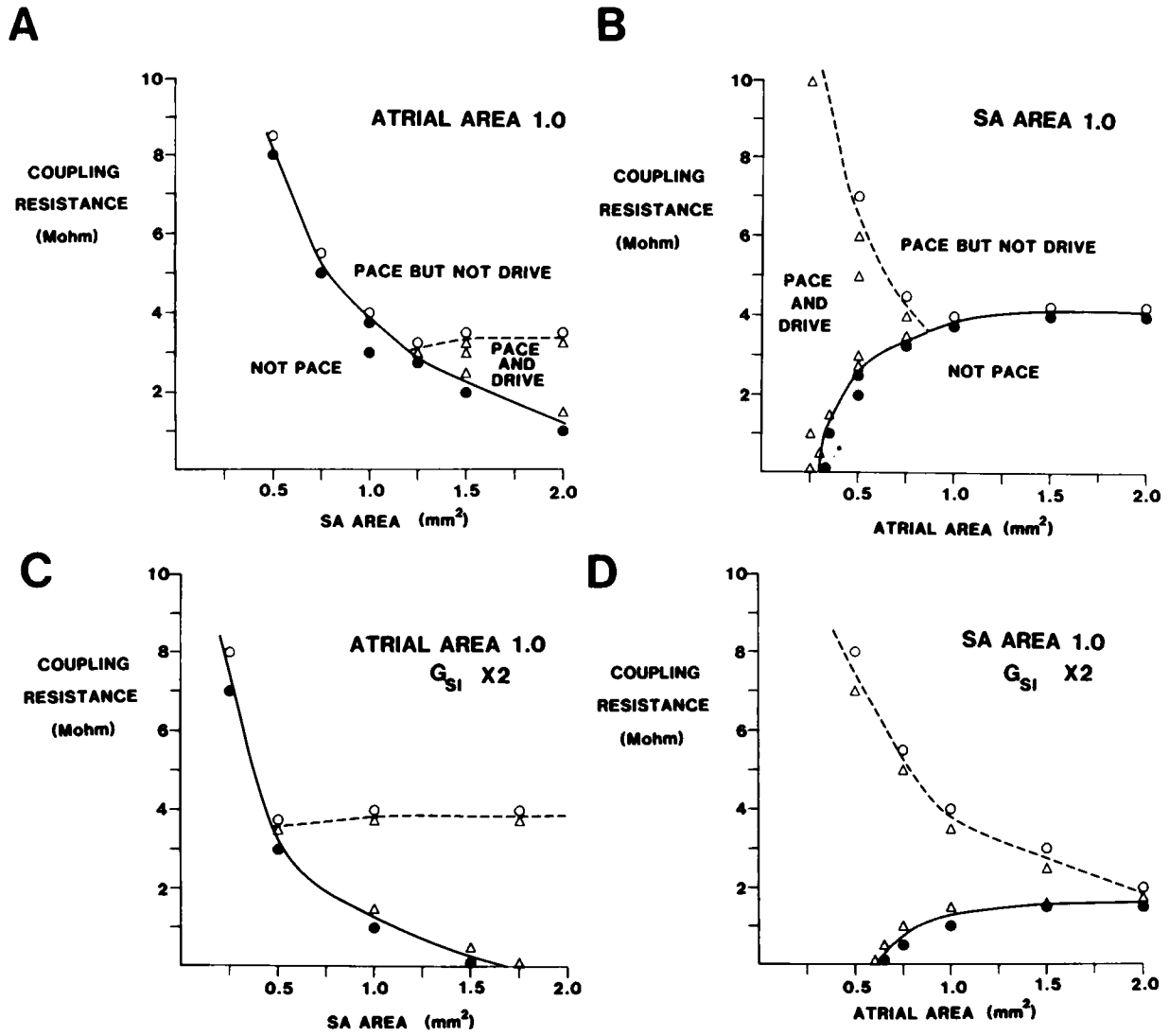

FIGURE 3 Simulated results for two electrically coupled membrane regions as in Fig. 2. Each symbol plotted represents a simulation of 2 s, with the simulation results being either: (*a*) failure of the SA region to pace (NOT PACE, ●), (*b*) pacing of the SA region without activation of the atrial region (PACE BUT NOT DRIVE, ○), or (*c*) pacing of the SA region with subsequent activation of the atrial region (PACE AND DRIVE, △). In *A* the membrane area of the atrial region is fixed at 1.0 mm², while the membrane area of the SA region and the coupling resistance are varied. In *B*, the membrane area of the SA region is fixed at 1.0 mm² while the membrane area of the atrial region and the coupling resistance are varied. The solid line separates the graph space into regions of pacing and not pacing. The dashed line separates the graph space into region of successful or unsuccessful driving of the atrial region. *C* and *D* correspond to *A* and *B*, respectively, except that the magnitude of the slow inward current is doubled for the SA region in *C* and *D*.

atrial membrane area region for the SA node to pace and drive the atrium. In *B*, we show the results of simulations in which we fixed the SA membrane area at 1 mm² and varied the atrial membrane area and R_c. There are again three regions of the graph corresponding to the three possible results. *C* and *D* show results for the same simulations as *A* and *B*, respectively, except that the magnitude of the conductance for the slow inward current, $G_{s.i.}$, has been increased by a factor of two in the SA membrane model. The region corresponding to successful pacing and driving has been considerably increased in size. Note that the solid line in all of the panels indicates the critical values of R_c for successful pacing, while the dashed line indicates the critical values of R_c for successful driving of the atrium if pacing of the SA node occurs. The major effect of the increased $G_{s.i.}$ in the SA region is clearly to increase the ability to pace even with the electrical load of the atrial membrane area present (shown by a downward shift in the solid lines of *C* and *D* as compared with *A* and *B*). Thus, while there are certainly some quantitative uncertainties in the membrane models used in these simulations, if one were to consider the real SA node and the surrounding atrial tissue as two directly coupled isopotential membrane regions, the SA node and atrial membrane areas would have to be about equal for successful pacing and driving to occur.

While there is some justification for considering the SA node region to be nearly isopotential, the atrial region clearly is not. Atrial cells at increasing distance from the SA node would have diminishing electrotonic interaction with the SA node. Thus it might be possible for a small SA node region to activate a much larger atrial region if the most proximal atrial cells could be directly excited by the SA node to initiate propagation through the atrium.

To evaluate this possibility we simulated a two-dimensional layer of cells with radial symmetry as was diagrammed in Fig. 1. We used 50 concentric circular elements, each 100-μm wide, and used a radius of 100 μm for the central circular element. We investigated the effects of the radial distribution of two variables. First, we varied the number of elements, starting from the center, which were represented by the SA node membrane model. For a simulation with N elements of the SA node model, we used $50 - N$ elements of the atrial model, making the effective radius of the SA node region $N \times 100$ μm. The total radius for each simulation was 50×100 μm = 5 mm. Second, we varied the radial distribution of intercellular resistivity. We assumed a value of 600 Ω cm (Bukauskas et al., 1982) as our "normal" value and investigated the effects of radial variation in this resistivity. Our results with two coupled cells showed that the coupling resistance affected both the ability of the SA cell to pace and its ability to drive the atrial cell. Fig. 4 shows some results with the distributed disk model. For the results shown in Figs. 4 and 5 we have two independent variables: the size of the SA node region and the resistivity (R_B, Ω cm) between the most peripheral SA node element and the most central atrial element. The radial resistivity was 600 Ω cm between all other elements. The variable resistivity, R_B, can be considered as a "barrier" resistance comparable to the resistance R_c for the two cell model, except that, for the disk model, R_B is between two distributed systems, whereas for the two cell model R_c is between two isopotential systems. Results of four simulations are shown in the four parts of Fig. 4. In each part, we plot the membrane potential as functions of time for elements 5, 10, 15, . . . 50 with a vertical offset of -20 mV for each successive element plotted. The voltage scale on the vertical axis is for the plot of element 5. Elements that are represented by the SA node model are indicated by an asterisk in all the plots. *A* and *B* of Fig. 4 have 25 SA node elements and 25 atrial elements. For *A* we used a barrier resistivity, R_B, of 4,000 Ω cm, whereas for *B* we used a value for R_B of 600 Ω cm, which makes the radial resistivity homogeneously 600 Ω cm throughout the disk. In both cases the SA region paces repetitivity but does not drive the surrounding atrial region. With the barrier resistivity of 4,000 Ω cm (*A*) the SA region paces more rapidly and there is less decrement of potential within the SA node region, as compared with *B* where no "barrier" is present. *C* and *D* of Fig. 4 are results of simulations identical to *A* and *B*, respectively, except that for *C* and *D* we used 30 SA node elements and 20 atrial elements, therefore making the SA node region larger. For *C* and *D* the SA region paces and also drives the atrial region.

The results obtained by systematically varying the number of SA node elements and the "barrier" resistivity, R_B, are shown in Fig. 5. Each symbol plotted represents a simulation using the radius of the SA node region as the abscissa and the value of R_B as the ordinate. The symbols have the same meaning as for the two cell results of Fig. 3. The three possible results (not pacing, pacing but not driving, pacing and driving) fall into three areas of the graph. The solid line separates regions of pacing and not pacing. The dashed line separates regions of driving and not driving. A major difference between these results for the distributed system and the results of Fig. 3 *A* for the two cell system is that these two lines do not intercept for the distributed system. The region of the graph labeled "PACE BUT NOT DRIVE" extends down to the R_B value of 600 Ω cm which is the condition of no resistance "barrier" at all. The mechanism for this effect is shown in Fig. 4 *B*. In this case, with no "barrier" resistance, the distributed nature of the SA node region allows the control part of the node to pace but the peripheral parts of the nodal region exhibit decremental conduction which fails to activate the surrounding atrial elements. The occurrence of this phenomenon in the distributed system produces a minimum radius of the SA node region (~2.3 mm) for successful driving of the atrium with the membrane models we used.

An alternative distribution of coupling resistivity is suggested by histological studies (Masson-Pevet et al., 1982) in which the frequency of occurrence of gap junctions among SA node cells is reported to be ~10% of the frequency of occurrence among atrial cells in the same preparations. Assuming that most of the intercellular resistance occurs at the gap junctions, this suggests that the radial resistivity throughout the SA node region might be as high as 6,000 Ω cm. This distribution of radial resistivity would provide greater electrical insulation of the central part of the SA node region from the atrial region than the discretely placed "barrier" of the simulation of Figs. 4 and 5. The results shown in Fig. 6 *A* were obtained by simulating a radial model as in Figs. 4 and 5 except that the radial resistivity was set at 6,000 Ω cm for the central 30 SA node elements and at 600 Ω for the peripheral 20 atrial elements. The SA node region paces at a high rate but fails to activate the atrial region. The problem with this resistivity distribution is that the short space constant within the SA node region allows only the most peripheral SA node elements to provide current to stimulate the atrial region. Thus an abrupt transition in resistive coupling would not allow the SA node region to function as both a pacing region and a sufficient source of current for the surrounding atrium. This suggests the need for a transitional region such that the high resistivity within the SA region allows a small region to pace but a gradual transi-

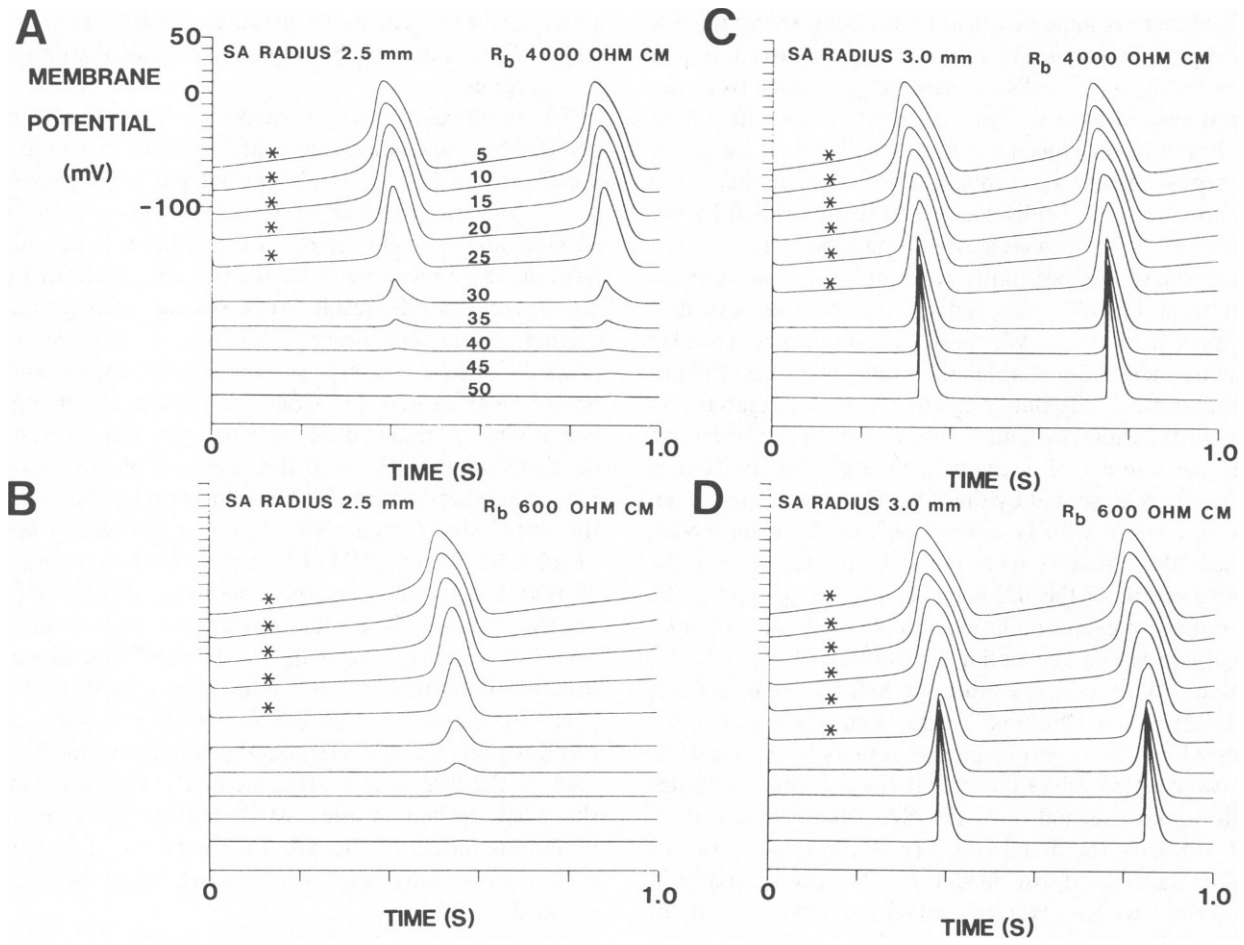

FIGURE 4 Results for simulations of the radially symmetric disk model of 50 elements. Each part (*A–D*) presents membrane potential as functions of time for elements 5, 10, 15, . . . 50 of the model. The vertical axis labels and scale of *A* apply to *B*, *C*, and *D* also. The voltage scale is for element 5, with subsequent elements plotted being displaced vertically by −20 mV for clarity. In *A* and *B*, the central 25 elements had the SA node membrane model, while the peripheral 25 elements had the atrial model. In *C* and *D* the central 30 elements had the SA node model and the peripheral 20 elements had the atrial model. The radial resistivity was 600 Ω cm between all elements except for *A* and *C* where the radial resistivity between the last SA node element and the first atrial elements was 4,000 Ω cm. *C* and *D* show successful propagation into the atrial region.

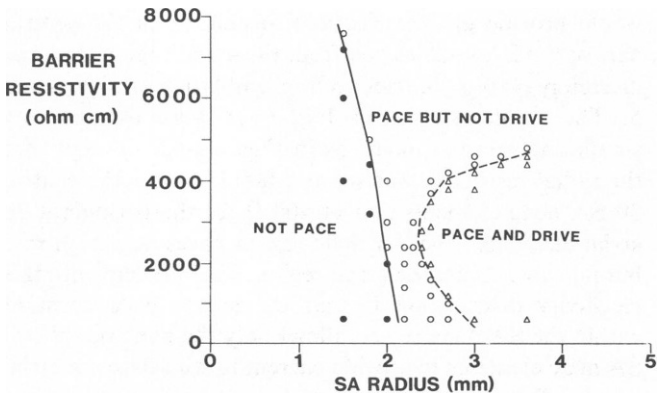

FIGURE 5 A summary of simulation results obtained with the radially symmetrical disk model. Each symbol plotted is the result of a simulation of 2 s and the symbol types (●, ○, and △) have the same meaning as in Fig. 3. The value of radial resistivity was 600 Ω cm between adjacent elements except for the presence of a "barrier resistivity" as shown between the most peripheral SA node element and the most central atrial element.

tion to the lower resistivity in the atrial region would allow propagation out into the atrial region.

Fig. 6 *B* was obtained by a simulation in which the SA model was used for only the central 10 elements. The radial resistivity was 6,000 Ω for those 10 elements, then linearly decreased over the next 10 elements to 600 Ω cm, and then remained at 600 Ω cm for the other 30 elements. The results show successful pacing at a rapid rate and successful propagation into the atrial region for this SA region with a radius of only 1 mm.

DISCUSSION

There is an important distinction to be made in regard to electrical properties of cells in an electrical syncytium. The intrinsic electrical properties (e.g., automaticity at a certain rate) are those properties that a particular cell would display in isolation from all other cells. These intrinsic electrical properties are assumed to be completely described by the mathematical model of membrane con-

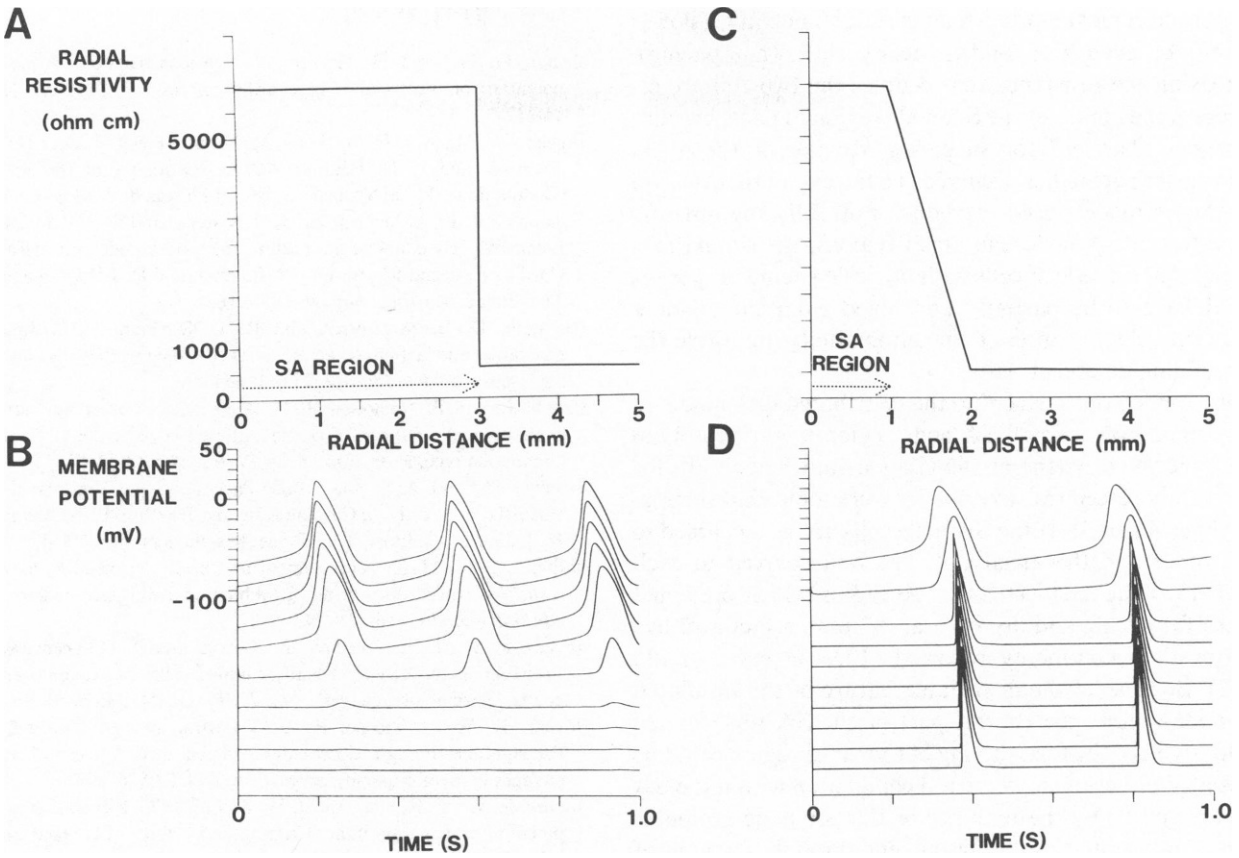

FIGURE 6 Results of two simulations with the radially symmetrical disk model in which the radial resistivity within the SA node region is 6,000 Ω cm. *A* and *C* are diagrams of two different radial distributions of radial resistivity and the SA node model. *B* and *D* are the simulation results for the distributions *A* and *C*, respectively.

ductances and capacitance. The expressed electrical properties are those that would be recorded from the cell within the syncytium, with all of the electrical interactions among the cells expressed as solutions of the cable equations that specify the current flow due to intercellular resistance coupling. Experimental work on strands of cardiac tissue, either Purkinje fibers (Antzelevitch et al., 1982) or rabbit SA node strips (Jalife, 1984) have demonstrated the importance of electrotonic modulation of the expressed electrical activity, particularly with regard to the expressed automatic rate being quite different from the intrinsic automatic rate of a pacing region.

Experimental measurements of junctional resistance between pairs of heart cells have been made using a double voltage clamp technique on pairs of dissociated rat ventricular cells. White et al. (1985) measured a junctional resistance of 10–100 MΩ, whereas Weingart (1986) measured values of 2 MΩ. Assuming a nonjunctional membrane resistance of 50 MΩ for each cell (Weingart, 1986) then the ratio of junctional resistance to nonjunctional resistance could be as low as 0.04 for a well-coupled electrical syncytium. Experimental work using pairs of cell aggregates (Clapham et al., 1980; Veenstra and deHaan, 1986) showed that synchronous activation of two aggregates with different intrinsic rates of automaticity could occur when the ratio of junctional to nonjunctional resistance was $< \sim 10$. Our simulations in Fig. 2 of two isopotential regions used a membrane area for each region of 1 mm^2. With the Beeler-Reuter model this corresponds to an input resistance (nonjunctional resistance) of ~0.5 MΩ while for the Irisawa-Noma model the nonjunctional resistance would be ~1.5 MΩ. Thus the junctional resistances of 2.5 or 5.0 MΩ we used represent a ratio of junctional to nonjunctional resistance in the range of 1.7–10, which is less than that required to synchronize two intrinsically pacing regions but much higher than would be expected for a well-coupled syncytium.

The simulations of two isopotential membrane regions, using published models for the respective membrane properties of SA node and atrial cells present a paradox in light of the published studies showing that the SA node is small compared to the surrounding atrial tissue, based on both electrophysiological mapping and histological studies. The SA node model is very sensitive to electrotonic influences during the diastolic depolarization because the membrane resistivity of the SA node model is high and the net inward current during this phase is small. Quiescent cells with more negative resting potential tend to block the pacing of electrically coupled SA node cells by current flow from the SA node cells into the quiescent atrial cells, making the net

membrane current of the SA node cell less negative (slower pacing) or even zero in the steady state (not pacing). Increasing the resistance that couples the two cell groups increases the ability of the SA node region to pace, but also creates a "barrier" for successful driving of the atrial region after pacing has occurred. To the extent that the two membrane models used reproduce faithfully the intrinsic properties of SA node and atrial regions, the simulations predict that a group of cells with intrinsic pacing properties would have to be partially uncoupled from surrounding quiescent cells to express their automaticity and drive the surrounding quiescent tissue

We applied this concept to the distributed disk model to understand how a small SA node region might be able to both pace and drive the surrounding atrium. The results for a discretely placed resistive barrier were somewhat surprising (Figs. 4 and 5). If the SA node cells are well coupled to each other and the atrial cells are well coupled to each other, then the smallest SA node radius which predicted successful pacing and driving was >2 mm, a factor of five greater than commonly reported (Masson-Pevet et al., 1982). Because of the distributed nature of the simulated SA node region, the central part of the SA node region could pace but the final driving of the atrial region could be prevented either by decremental conduction within the SA node region or by the inability of the SA node region to supply sufficient stimulating current through a region of higher resistivity.

When we included the histological data of a 90% reduction in gap junction frequency within the SA node region this allowed a much smaller SA node region to pace and drive the surrounding atrial region (Fig. 6). However, this effect of reducing the required SA node size was only present if there was a transitional zone of gradual decrease in radial resistivity. When an abrupt transition was present, the increased cell–cell resistive coupling in the SA node region actually produced an increase in the required SA node size.

In this work we have not assumed any gradual transition in intrinsic membrane properties. We suspect that just as the gradual transition in cell–cell resistivity, a gradual transition in membrane properties might help to explain the ability of the small central nodal region to function. Recent experiments by Kodama and Boyett (1985) have shown a gradual transition in membrane properties in small isopotential cell groups isolated at increasing distances from the central SA node region. Both the regional specification of membrane properties and the incorporation of the results into a two dimensional model without radial symmetry should help to further explain the SA node–atrial interactions.

This work was supported in part by National Institutes of Health grant HL-22562 to Dr. Joyner.

Received for publication 17 March 1986 and in final form 13 June 1986.

REFERENCES

Beeler, G. W., and H. Reuter. 1977. Reconstruction of the action potential of ventricular myocardial fibres. *J. Physiol. (Lond.)*. 268:177–210.

Bleeker, W. M., A. J. C. Mackaay, M. Masson-Pevet, T. Op't-Hof, H. J. Jongsma, and L. N. Bouman. 1982. Asymmetry of the sino-atrial conduction in the rabbit heart. *J. Mol. Cell. Cardiol.* 14:633–643.

Bukauskas, F. F., A. M. Gutman, K. J. Kisunas, and R. P. Veteikis. 1982. Electrical cell coupling in rabbit sino atrial node and atrium. *In* Cardiac Rate and Rhythm. L. N. Bouman and H. J. Jongsma, editors. The Hague: Martinus Nijhoff. 195–216.

Clapham, D. E., A. Shrier, and R. L. DeHaan. 1980. Junctional resistance and action potential delay between embryonic heart cell aggregates. *J. Gen. Physiol.* 75:651–654.

Crank, J., and P. Nicholson. 1947. A practical method for numerical evaluation of solutions of partial differential equations of the heat-conduction type. *Proc. Cambridge Philos. Soc.* 43:50–67.

Irisawa, H., and A. Noma. 1982. Pacemaker mechanisms of rabbit sinoatrial node cells. *In* Cardiac Rate and Rhythm. L. N. Bouman and H. J. Jongsma, editors. The Hague: Martinus Nijhoff. 35–52.

Jalife, J. 1984. Mutual entrainment and electrical coupling as mechanisms for synchronous firing of rabbit sino-atrial pace-maker cells. *J. Physiol. (Lond.)*. 356:221–243.

Joyner, R. W., E. D. Overholt, B. Ramza, and R. D. Veenstra. 1984. Propagation through electrically coupled cells: two inhomogeneously coupled cardiac tissue layers. *Am. J. Physiol.* 247:H596–H609.

Joyner, R. W., J. Picone, R. D. Veenstra, and D. Rawling. 1983. Propagation through electrically coupled cells: effects of regional changes in membrane properties. *Circ. Res.* 53:526–534.

Joyner, R. W., F. Ramon, and J. W. Moore. 1975. Simulation of action potential propagation in an inhomogeneous sheet of coupled excitable cells. *Circ. Res.* 36:654–661.

Joyner, R. W., M. Westerfield, J. W. Moore, and N. Stockbridge. 1978. A numerical method to model excitable cells. *Biophys. J.* 22:155–170.

Kodama, I., and M. R. Boyette. 1985. Regional differences in the electrical activity of the rabbit sinus node. *Pflug. Arch.* 404:214–226.

Mackaay, A. J. C., T. Op't-Hof, W. K. Bleeker, H. J. Jongsma, and L. N. Bouman. 1980. Interaction of adrenaline and acetylcholine on cardiac Pacemaker function. Functional inhomogeneity of the rabbit sinus node. *J. Pharmacol. Exp. Ther.* 214:417–422.

Masson-Pevet, M., W. K. Bleeker, and D. Gros. 1979. The plasma membrane of leading pacemaker cells in the rabbit sinus node: a qualitative and quantitative ultrastructural analysis. *Circ. Res.* 45:621–629.

Masson-Pevet, M. A. W. K. Bleeker, E. Besselsen, A. J. C. Mackaay, H. J. Jongsma, and L. N. Bouman. 1982. On the ultrastructural identification of pacemaker cell types. *In* Cardiac Rate and Rhythm. L. N. Bouman and H. J. Jongsma. The Hague: Martinus Nijhoff. 19–34.

Moore, J. W., F. Ramon, and R. W. Joyner. 1975. Axon voltage-clamp simulations. I. Methods and tests. *Biophys. J.* 15:11–23.

Sharp, G. H., and R. W. Joyner. 1980. Simulated propagation of cardiac action potentials. *Biophys. J.* 31:403–424.

Sommer, J. R., and E. A. Johnson. 1979. Ultrastructure of cardiac muscle. *In* Handbook of Physiology. Sec. 2. The Cardiovascular System, Vol. I. The Heart. R. M. Berne, N. Sperelakis, and S. Geiger, editors. American Physiological Society, Wash. DC. 113–186.

Twizell, E. H. 1984. Computational methods for partial differential equations. Chapter 5. John Wiley & Sons, Inc. New York. 200–265.

Veenstra, R. D., and R. L. DeHaan. 1986. Electrotonic interactions between aggregates of chick embryo cardiac pacemaker cells. *Am. J. Physiol.* 250:H453–H463.

Weingart, R. 1986. Electrical properties of the nexal membrane studied in rat ventricular cell pairs. *J. Physiol. (Lond.)* 370:267–284.

White, R. L., D. C. Spray, A. C. Campos de Carvalho, B. A. Wittenberg, and M. V. L. Bennett. 1985. Some electrical and pharmacoligical properties of gap junctions between adult ventricular myocytes. *Am. J. Physiol.* 249:C447–C455.